



STATE RESEARCH CENTER OF RUSSIA  
INSTITUTE FOR HIGH ENERGY PHYSICS

IHEP 2010-4

N.M. Agababyan <sup>1</sup>, V.V. Ammosov, N. Grigoryan <sup>2</sup>,  
H. Gulkanyan <sup>2</sup>, A.A. Ivanilov <sup>\*</sup>, Zh. Karamyan <sup>2</sup>,  
V.A. Korotkov

**THE YIELDS OF LIGHT MESON RESONANCES  
IN NEUTRINO-NUCLEUS INTERACTIONS  
AT  $\langle E_\nu \rangle \approx 10$  GeV**

Submitted to *Yad. Fiz.*

---

<sup>1</sup>) Joint Institute for Nuclear Research, Dubna, Russia

<sup>2</sup>) Yerevan Physics Institute, Armenia

<sup>\*</sup> E-mail: ivanilov@mx.ihep.su

**Abstract**

Agababyan N.M., Grigoryan N., Ivanilov A.A. et al. The Yields of Light Meson Resonances in Neutrino-Nucleus Interactions at  $\langle E_\nu \rangle \approx 10$  GeV: IHEP Preprint 2010-4. – Protvino, 2010. – p. 15, figs. 7, tables 4, refs.: 23.

The total yields of the all well established light meson resonances (up to the  $\phi(1020)$  meson) are estimated in neutrino-nucleus charged current interactions at  $\langle E_\nu \rangle \approx 10$  GeV, using the data obtained with SKAT bubble chamber. The yield of  $\phi$  meson in neutrino production is obtained for the first time. For some resonances, the yields in the forward and backward hemispheres in the hadronic c.m.s. are also extracted. From the comparison of the obtained and available higher energy data, an indication is obtained that the resonance yields rise almost linearly as a function of the mass  $W$  of the neutrino produced hadronic system. The fractions of pions originating from the light resonance decays are inferred.

**Аннотация**

Агабабян Н.М., Григорян Н., Иванчиков А.А. и др. Выходы легких мезонных резонансов в нейтрино-ядерных взаимодействиях при  $\langle E_\nu \rangle \approx 10$  ГэВ: Препринт ИФВЭ 2010-4. – Протвино, 2010. – 15 с., 7 рис., 4 табл., библиогр.: 23.

Используя данные, полученные с помощью пузырьковой камеры SKAT, оценены выходы всех хорошо установленных легких мезонных резонансов (вплоть до  $\phi(1020)$ -мезона) в нейтрино-ядерных взаимодействиях через заряженный ток при  $\langle E_\nu \rangle \approx 10$  ГэВ. Выход  $\phi$ -мезона в нейтринорождении получен впервые. Для некоторых резонансов получены также выходы в направлениях передней и задней полусфер в с.ц.м. адронов. Из сравнения полученных и имеющихся данных получено указание на то, что выходы резонансов растут приблизительно линейно как функция массы  $W$  адронной системы, образованной в нейтрино-ядерных взаимодействиях. Получено значение доли  $\pi$ -мезонов от распада легких мезонных резонансов.

## 1. INTRODUCTION

The space-time pattern of the leptoproduced quark-string fragmentation into hadrons would be rather incomplete without discerning to what extent the hadrons detected in a given phase-space domain originate directly from the string fragmentation and to what they are decay products of other, higher mass string fragments—resonances. Although it is generally accepted that the later cause a significant fraction of the yields of stable hadrons (pions and kaons), a quantitative estimation of this fraction is not available yet, at least for neutrino induced reactions. At present, more or less detailed experimental data on the neutrino production of meson resonances are available for  $\rho$  mesons ([1, 2, 3, 4, 5] and references therein), and for charged  $K^*(892)$  mesons ([6, 7] and references therein), while those for other resonances are rather scarce and obtained at high energies of (anti)neutrino,  $\langle E_\nu \rangle \sim 40\text{-}50$  GeV [2]. The aim of this work is to measure, at the same experimental conditions, the yields of the all well-established light meson resonances (with masses up to  $\sim 1$  GeV/ $c^2$ ) in neutrino-nucleus charged current interactions at intermediate energies ( $\langle E_\nu \rangle \sim 10$  GeV). In Section 2, the experimental procedure is described. Section 3 presents the experimental data on the total yields of 12 meson resonances:  $\eta$ ,  $\rho^0$ ,  $\rho^+$ ,  $\rho^-$ ,  $\omega$ ,  $K^*(892)^0$ ,  $\bar{K}^*(892)^0$ ,  $K^*(892)^+$ ,  $K^*(892)^-$ ,  $\eta'(958)$ ,  $f_0(980)$  and  $\phi$ . For some cases, the differential yields in the forward and backward hemispheres (in the hadronic c.m.s.) are also presented. The dependence of the resonance yields on their mass and the invariant mass  $W$  of the created hadronic system is compared to the higher energy neutrino production and  $e^+e^-$  annihilation data. Section 4 is devoted to the estimation of the fraction of pions originating from the decays of the light meson resonances. The results are summarized in Section 5.

## 2. EXPERIMENTAL PROCEDURE

The experiment was performed with SKAT bubble chamber [8], exposed to a wideband neutrino beam obtained with a 70 GeV primary protons from the Serpukhov accelerator.

The chamber was filled with a propane-freon mixture containing 87 vol% propane ( $C_3H_8$ ) and 13 vol% freon ( $CF_3Br$ ) with the percentage of nuclei H:C:F:Br = 67.9:26.8:4.0:1.3 %. A 20-kG uniform magnetic field was provided within the operating chamber volume.

Charged current interactions containing a negative muon with momentum  $p_\mu > 0.5$  GeV/c were selected. Other negatively charged particles were considered to be  $\pi^-$  mesons, except for the cases explained below. Protons with momentum below 0.6 GeV/c and a fraction of protons with momentum 0.60–0.85 GeV/c were identified by their stopping in the chamber. Non-identified positively charged particles were considered to be  $\pi^+$  mesons, except for the cases explained below. Events in which errors in measuring the momenta of all charged secondaries and photons were less than 60% and 100%, respectively, were selected. The mean relative error  $\langle \Delta p/p \rangle$  in the momentum measurement for muons, pions and gammas was, respectively, 3%, 6.5% and 19%. Each event is given a weight which corrects for the fraction of events excluded due to improperly reconstruction. More details concerning the experimental procedure, in particular, the estimation of the neutrino energy  $E_\nu$  and the reconstruction of  $\pi^0 \rightarrow 2\gamma$  decays can be found in our previous publications [9, 5]. The events with  $3 < E_\nu < 30$  GeV were accepted, provided that the reconstructed mass  $W$  of the hadronic system exceeds 1.8 GeV. No restriction was imposed on the transfer momentum squared  $Q^2$ . The number of accepted events was 5242 (6557 weighted events). The mean values of the kinematic variables were  $\langle E_\nu \rangle = 9.8$  GeV,  $\langle W \rangle = 2.8$  GeV,  $\langle W^2 \rangle = 8.7$  GeV<sup>2</sup>,  $\langle Q^2 \rangle = 2.6$  (GeV/c)<sup>2</sup>.

About 8% of neutrino interactions occur on free hydrogen. This contribution was subtracted using the method described in [10, 11]. The effective atomic weight of the composite nuclear target is estimated [9] to be approximately equal to  $A_{\text{eff}} = 21 \pm 2$ , thus allowing to compare our results with those obtained in  $\nu(\bar{\nu})Ne$  interactions at higher energies [2].

When considering the production of resonances decaying into charged kaon(s), the  $K^-$  and  $K^+$  hypothesis was applied, respectively, for negatively charged particles and non-identified positively charged particles (provided that the kaon hypothesis is not rejected by the momentum-range relation in the propane-freon mixture), introducing thereat proper corrections for the momentum of these particles.

### 3. EXPERIMENTAL RESULTS

#### *3.1. The Experimental Mass Resolutions and the Fitting Procedure of Mass Distributions*

The experimental mass resolutions for different resonances are estimated from Monte-Carlo simulations, in which the Breit-Wigner function [12] is smeared taking into account the experimental resolution. The FWHM (full width at half maximum) values  $\Gamma_{\text{exp}}^R$  of simulated distributions are presented in Table 1. In the cases, when  $\Gamma_{\text{exp}}^R$  significantly exceeds the resonance natural width,  $\Gamma_0^R$ , the mass distributions were fitted as a sum of the background ( $BG(m)$ ) and Gaussian ( $G_R(m)$ ) distributions,

$$dN/dm = \text{BG}(m) + \alpha_R G_R(m) , \quad (1)$$

where for the Gaussian width  $\sigma_R$  the following relation was used:  $\Gamma_{\text{exp}}^R = 2\sigma_R\sqrt{2\ln 2}$ . Otherwise, the mass distributions were fitted by the form

$$dN/dm = \text{BG}(m) \cdot (1 + \alpha_R \text{BW}_R(m)) , \quad (2)$$

where  $\text{BW}_R(m)$  is the corresponding Breit-Wigner function, with  $\Gamma_0^R$  replaced by an effective  $\Gamma_{\text{exp}}^R$ .

The background distribution was parametrized as

$$\text{BG}(m) = B \cdot (m - m_{\text{th}})^\beta \exp\left(\sum_{i=1}^k \varepsilon_i m^i\right) , \quad (3)$$

where  $m_{\text{th}}$  is the threshold mass of the corresponding resonance;  $k = 1$  or  $2$ , depending on the statistics;  $B$ ,  $\beta$  and  $\varepsilon_i (i = 1, k)$  are fit parameters. In some cases, depending on the form of the mass distribution, the parameter  $\beta$  was fixed to 0.

The form (1) was applied for  $\eta$ ,  $\omega$ ,  $\eta'$  and  $\phi$ , while the form (2) was used for  $\rho^0$ ,  $\rho^\pm$ ,  $K^*(892)^0$  and  $K^*(892)^\pm$ . For  $f_0(980)$ , for which  $\Gamma_{\text{exp}}^R$  does not much exceed its natural width  $\Gamma_0^f = 35$  MeV (taken from a recent NOMAD measurement [3]), both (1) and (2) forms were used, leading to compatible results. The pole mass of  $f_0(980)$ ,  $m_{f_0} = 963$  MeV, was also taken from [3], while for other resonances considered in this paper the masses and widths are fixed according to the PDG values [13].

**Table 1.** The experimental mass resolutions for different resonances

resonance	$\rho^0$	$f_0$	$\rho^\pm$	$\eta$	$\omega$	$\eta'$	$K^{*0}$	$K^{*\pm}$	$\phi$
decay mode	$\pi^+\pi^-$	$\pi^+\pi^-$	$\pi^\pm\pi^0$	$\pi^+\pi^-\pi^0$	$\pi^+\pi^-\pi^0$	$\pi^+\pi^-\gamma$	$K^\pm\pi^\mp$	$K_s^0\pi^\pm$	$K^+K^-$
$\Gamma_{\text{exp}}^R$ (MeV)	47	55	110	66	90	100	28	30	10

### 3.2. Non-strange Resonances

The  $(\pi^+\pi^-)$  effective mass distribution is plotted in Figure 1 (the left panels) for the whole range of the Feynman  $x_F$  variable, as well as for the forward ( $x_F > 0$ ) and backward ( $x_F < 0$ ) hemispheres in the hadronic c.m.s. Signals for  $\rho^0$  and  $f_0(980)$  production are visible, except for  $f_0(980)$  at  $x_F < 0$ . The corresponding mean multiplicities are quoted in Table 2 (the data on  $f_0(980)$  are corrected for the  $\pi^+\pi^-$  decay fraction). These values are, as expected, somewhat smaller than those estimated recently [4] at a slightly severe cut on  $W$  ( $W > 2$  instead of  $W > 1.8$  GeV, or  $\langle W \rangle = 3.0$  instead of  $\langle W \rangle = 2.8$  GeV). As it is seen from Table 2, the  $\rho^0$  and  $f_0(980)$  production occurs predominantly in the forward hemisphere.

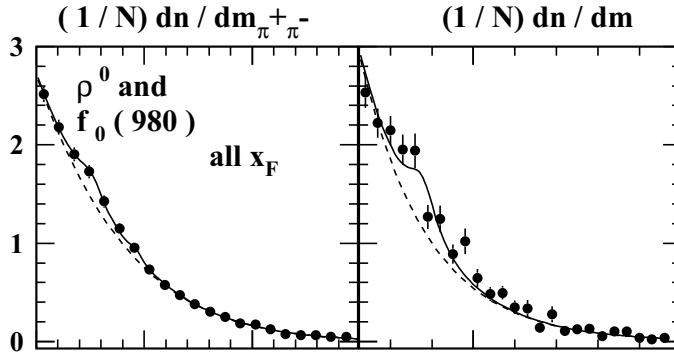


Figure 1. The effective mass distributions for systems  $\pi^+\pi^-$ ,  $\pi^+\gamma\gamma$  and  $\pi^-\gamma\gamma$ . The solid and dashed curves are the fit results for experimental and background distributions.

The total yields of charged  $\rho$  mesons and the differential yields of  $\rho^+$  at  $x_F > 0$  and  $x_F < 0$  were measured in our previous work [5] where the same cut  $W > 1.8$  GeV was applied as in the present study. In this work, an attempt is undertaken to estimate the  $\rho^-$  yields at  $x_F > 0$  and  $x_F < 0$  too. Figure 1 shows the effective mass distributions for  $\pi^+\gamma\gamma$  and  $\pi^-\gamma\gamma$  systems. The distributions are corrected for losses of reconstructed  $\pi^0$  and contamination from the background  $\gamma\gamma$  combinations (see [5] for details). The  $\rho^-$  signal is observable at  $x_F < 0$ , but not at  $x_F > 0$ , occupied mainly by favored mesons which can, unlike  $\rho^-$  meson, contain the current quark. The total and differential yields of  $\rho^+$  and  $\rho^-$  are quoted in Table 2.

**Table 2.** The mean multiplicities of light resonances

resonance	all $x_F$	$x_F > 0$	$x_F < 0$
$\eta$	$0.050 \pm 0.044$	$0.051 \pm 0.027$	$0.015 \pm 0.030$
$\rho^0$	$0.054 \pm 0.017$	$0.042 \pm 0.015$	$0.013 \pm 0.009$
$\rho^+$	$0.120 \pm 0.031$	$0.051 \pm 0.015$	$0.067 \pm 0.025$
$\rho^-$	$0.039 \pm 0.015$	$0.010 \pm 0.008$	$0.031 \pm 0.013$
$\omega$	$0.053 \pm 0.017$	$0.044 \pm 0.012$	$0.005 \pm 0.013$
$\eta'(958)$	$0.025 \pm 0.020$	$0.016 \pm 0.010$	$0.009 \pm 0.016$
$f_0(980)$	$0.014 \pm 0.010$	$0.012 \pm 0.008$	$0.002 \pm 0.009$
$K^*(892)^0$	$0.023 \pm 0.013$	$0.002 \pm 0.008$	$0.020 \pm 0.012$
$\bar{K}^*(892)^0$	$0.015 \pm 0.010$	$0.001 \pm 0.007$	$0.016 \pm 0.010$
$K^*(892)^+$	$0.022 \pm 0.012$	$0.012 \pm 0.010$	—
$K^*(892)^-$	$0.006 \pm 0.005$	—	—
$\phi(1020)$	$0.009 \pm 0.006$	$0.008 \pm 0.003$	$0.002 \pm 0.004$

The signals for  $\eta$  and  $\omega$  production were looked for in decays  $\eta \rightarrow \pi^+\pi^-\pi^0$  (with 22.7% decay fraction) and  $\omega \rightarrow \pi^+\pi^-\pi^0$  (with 89% decay fraction). The  $\pi^+\pi^-\gamma\gamma$  effective mass distributions in three  $x_F$ -ranges are plotted in Figure 2 (the left panels). As for the case of  $\rho^\pm$  [5], the distributions are corrected for losses of reconstructed  $\pi^0$  and the background  $\gamma\gamma$  contamination. It is seen from Figure 2 and Table 2 that, as in the case of  $\rho^0$ , the yields of  $\eta$  and  $\omega$  are strongly suppressed at  $x_F < 0$  as compared to those in the forward hemisphere. A similar pattern was observed earlier in  $\nu(\bar{\nu}) - Ne$  interactions at higher energies [2].

The production of  $\eta'$  was looked for in the channel  $\eta' \rightarrow \rho^0\gamma \rightarrow \pi^+\pi^-\gamma$  (with the decay fraction 29.4%, including the non-resonant  $\pi^+\pi^-$  background). The effective mass of the  $(\pi^+\pi^-)$ -system was restricted to the  $\rho^0$  mass range 0.6-0.9 GeV/ $c^2$ , these boundaries being close to those applied in other experiments in which the  $\eta' \rightarrow \rho^0\gamma$  decay fraction had been measured (see references in [13]). The  $\pi^+\pi^-\gamma$  effective mass distributions, corrected for the  $\gamma$  detection efficiency, are plotted in Figure 2 (the right panels). Rather faint signals for  $\eta'$  production are visible, more significant at  $x_F > 0$ . The estimated corresponding yields corrected for the decay fraction are presented in Table 2. Note, that the yield of  $\eta'$  at  $x_F > 0$  is significantly smaller as compared to that for  $\eta$ , composing  $(31 \pm 25)\%$  of the latter.

### 3.3. Strange Resonances

The production of  $K^*(892)^0$  and  $\bar{K}^*(892)^0$  was looked for in channels  $K^+\pi^-$  and  $K^-\pi^+$ , respectively. The main problem to separate these resonances is the large background from pion pairs in which the kaon hypothesis is applied for one of pions. The

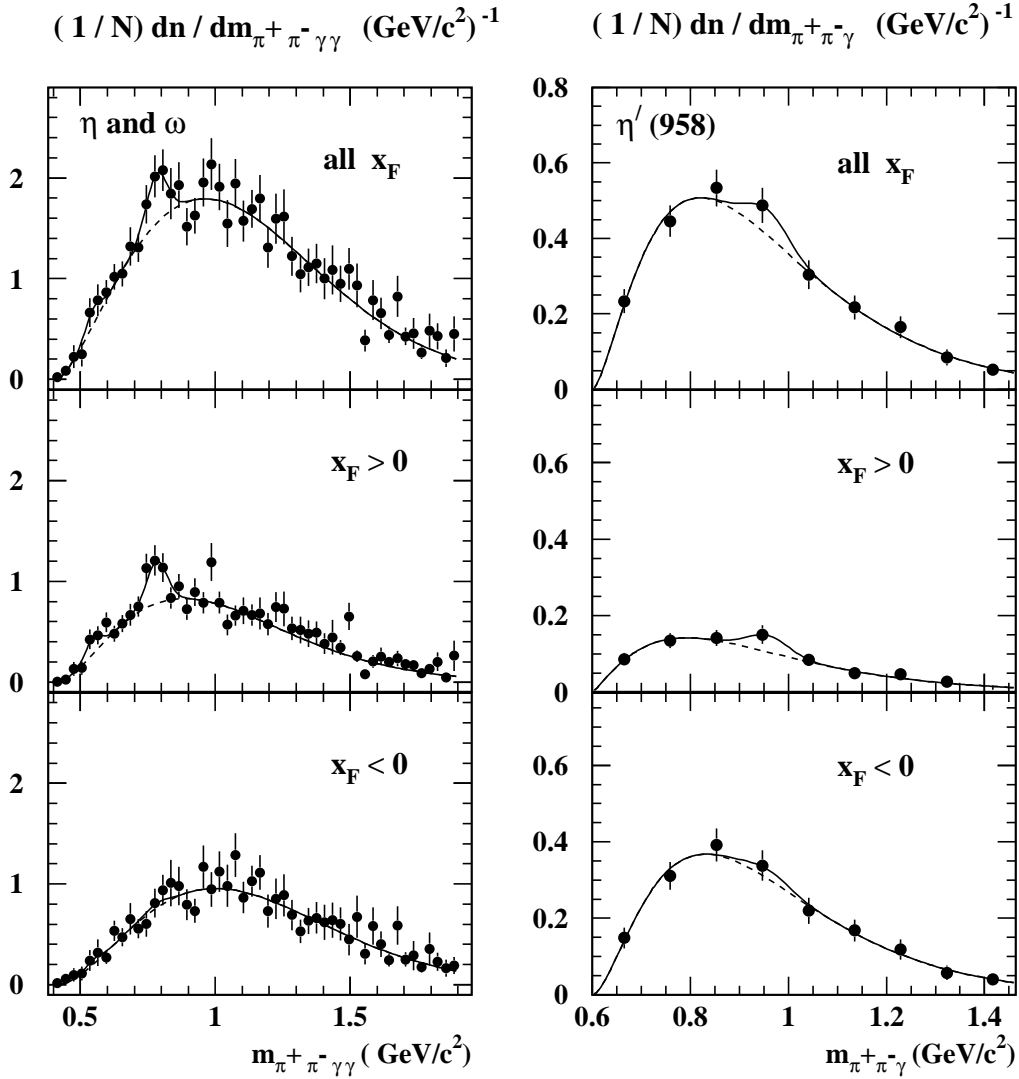


Figure 2. The effective mass distributions for systems  $\pi^+\pi^-\gamma\gamma$  and  $\pi^+\pi^-\gamma$ . The explanation of curves is the same as for Figure 1.

background from uncorrelated ( $\pi^+\pi^-$ ) can be approximated by a smooth curve (according to eq.(3)), while the background from correlated  $\pi^+\pi^-$ , originating from the decay of the same parent particle, can induce peculiarities in the effective mass spectra calculated for ( $K\pi$ ) hypothesis. To subtract the correlated background from  $\eta \rightarrow \pi^+\pi^-\pi^0$ ,  $\omega \rightarrow \pi^+\pi^-\pi^0$  and  $\rho^0 \rightarrow \pi^+\pi^-$  decays, we calculated, using their yields extracted in this work, their contributions to the ( $\pi^+\pi^-$ ) mass spectrum. Then each ( $K\pi$ ) combination was weighted, depending on the mass of the corresponding ( $\pi^+\pi^-$ ) pair. In a similar way,



we took also into account the contribution from the non-identified  $K_s^0 \rightarrow \pi^+\pi^-$  decays at very close distances from the neutrino interaction vertex (the magnitude of these 'close' decays was estimated from the analysis of  $(\pi^+\pi^-)$  mass spectrum).

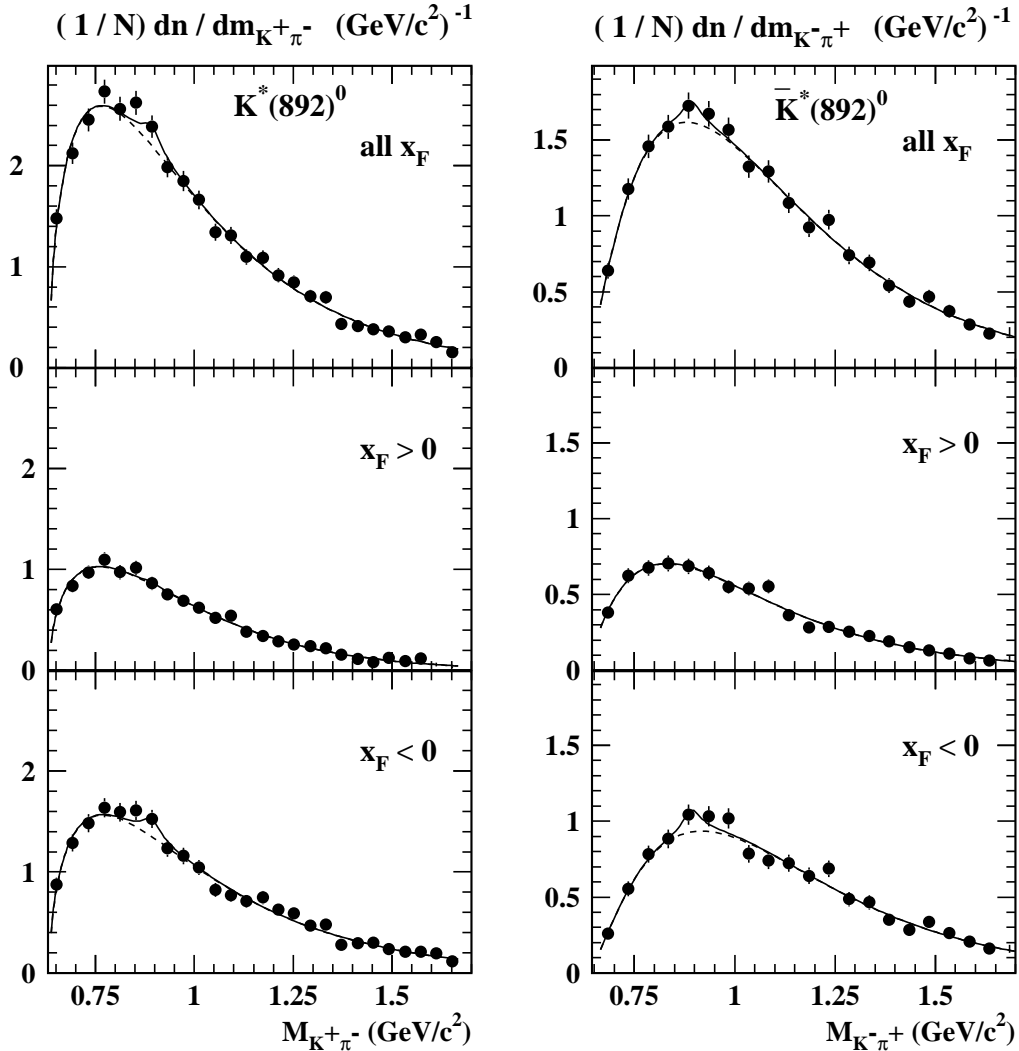


Figure 3. The effective mass distributions for systems  $K^+\pi^-$  and  $K^-\pi^+$ . The explanation of curves is the same as for Figure 1.

The effective mass spectra for  $(K^+\pi^-)$  and  $(K^-\pi^+)$ , corrected as described above, are plotted in Figure 3, while the estimated yields of  $K^*(892)^0$  and  $\bar{K}^*(892)^0$  (corrected for the decay fractions) are presented in Table 2. Despite of large relative errors, one can deduce that the yield of these resonances at  $x_F > 0$  is suppressed as compared to that at  $x_F < 0$ . This can be a direct consequence of their valence quark composition,  $K^{*0}(d\bar{s})$

and  $\bar{K}^{*0}(\bar{d}s)$ . As it can be estimated from the parton model (following [14, 15, 16]), the probability of creation of favored  $K^{*0}$  and  $\bar{K}^{*0}$  initiated by sub-processes  $\nu\bar{u} \rightarrow \mu^-\bar{s}$  and  $\nu\bar{u} \rightarrow \mu^-\bar{d}$ , respectively, and carrying relatively large positive  $x_F$ 's, is much smaller, than that for unfavored ones produced in the region of  $x_F < 0$ , as a result of the fragmentation of the quark string formed in the main sub-process  $\nu d \rightarrow \mu^-u$ .

The production of  $K^*(892)^\pm$  was looked for in channels  $K_s^0\pi^\pm$ . The effective mass distributions of the  $(K_s^0\pi^+)$  and  $(K_s^0\pi^-)$  systems for the full  $x_F$ -range and of the  $(K_s^0\pi^+)$  system at  $x_F > 0$  are plotted in Figure 4 (the left panels). The shape of the background distributions was determined with the help of the mixed event technique, combining  $K_s^0$ 's with  $\pi$  mesons from other events in which another  $K_s^0$  was detected. The parameters of the background distribution were fixed from the fit by eq. (3), except the normalization parameter  $B$  which was considered as a free parameter when fitting the experimental distribution by eq. (2). The fit results for the mean multiplicities (corrected for the decay fractions) are presented in Table 2. Due to the smallness of the  $K_s^0$  statistics, no estimations for yields can be inferred separately at  $x_F > 0$  and/or  $x_F < 0$ .

If one assumes, that the ratio  $R_V(S/N)$  of the summary total yields of strange ( $K^{*0}$ ,  $\bar{K}^{*0}$ ,  $K^{*+}$ ,  $K^{*-}$ ) and non-strange ( $\rho^0$ ,  $\rho^+$ ,  $\rho^-$ ,  $\omega$ ) vector mesons is not significantly influenced by the contribution from the higher mass resonances decaying into these mesons, the  $R_V(S/N)$  can be considered as an approximate measure of the strangeness suppression in the quark string fragmentation process. Using the data quoted in Table 2, one obtains  $R_V(S/N) = 0.25 \pm 0.09$ . This estimate is compatible with the values of the strangeness suppression factor  $\lambda_s$  inferred from different experiments using various methods (see [17, 18, 19, 20, 21], as well as our recent work [5]).

### 3.4. $\phi(1020)$ Meson

The  $(K^+K^-)$  effective mass distribution for different ranges of  $x_F$  are plotted in Figure 4 (the right panel). The contamination from correlated  $(\pi^+\pi^-)$  pair was subtracted as described in the previous subsection. The  $\phi$  yields corrected for the decay fraction are presented in Table 2. As it is seen, the production of the  $\phi$  mesons occurs, in contrast to the open strangeness  $K^*(892)^0$  and  $\bar{K}^*(892)^0$  mesons, only in the forward hemisphere. This can happen if the  $\phi$  meson is a decay product of a favored meson carrying a significant fraction of the hadrons energy. The most probable candidate is the charmed, strange meson  $D_s^+$  created directly as a result of the sub-process  $\nu s \rightarrow \mu^-c$  followed by the recombination of the current charmed quark with the strange antiquark from the nucleon remnant, or created indirectly as a result of the decay of the favored  $D_s^{*+}$  meson,  $D_s^{*+} \rightarrow D_s^+\gamma$ . The later process (for the case of  $D_s^{*-}$ ) was observed, with a appreciably large probability (about 5%), in charged current  $\bar{\nu}Ne$  interactions [22].

The data on the  $\phi$  neutrino production is obtained for the first time. The results of a more detailed analysis of our experimental data on the  $\phi$  neutrino production will be published elsewhere.

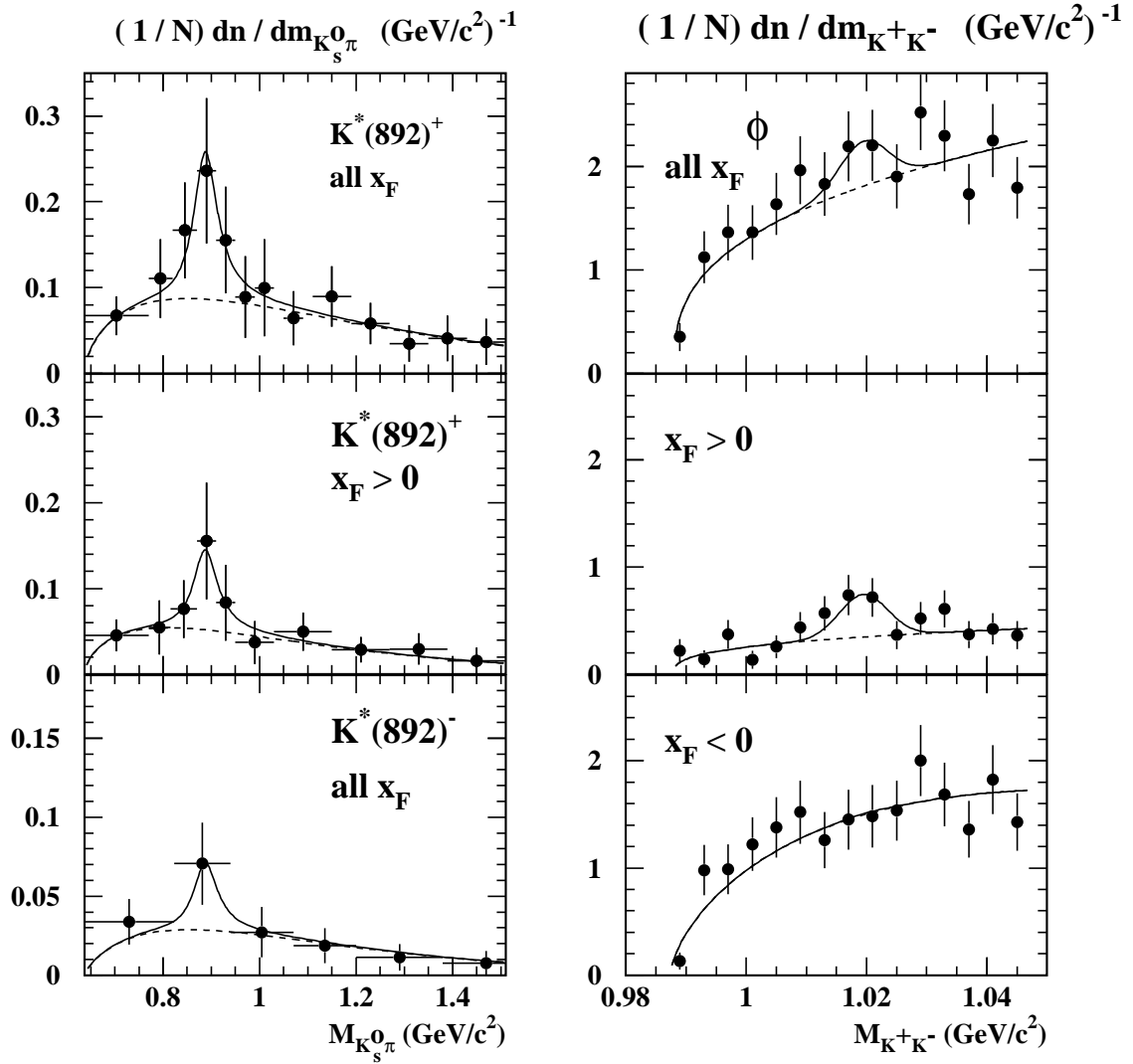


Figure 4. The effective mass distributions for systems  $K_s^0\pi^+$ ,  $K_s^0\pi^-$  and  $K^+K^-$ . The explanation of curves is the same as for Figure 1.

### 3.5. The $W$ -Dependence of the Resonance Yields

Our data on  $\eta$ ,  $\rho$  and  $\omega$  neutrino production (at  $W = 2.8$  and  $3.0$  GeV) combined with those obtained in  $\nu(\bar{\nu})Ne$  interactions at higher energies at  $W = 1.5 - 10.0$  GeV [2], as well as the data on  $K^*(892)^+$  neutrino production ([6] and references therein) allow one to trace the  $W$ -dependence of the yields of these resonances plotted in Figure 5. These dependencies can be approximately described by a simplest linear form  $b \cdot (W - W_0)$  at the fixed threshold value  $W_0 = 1.8$  GeV.

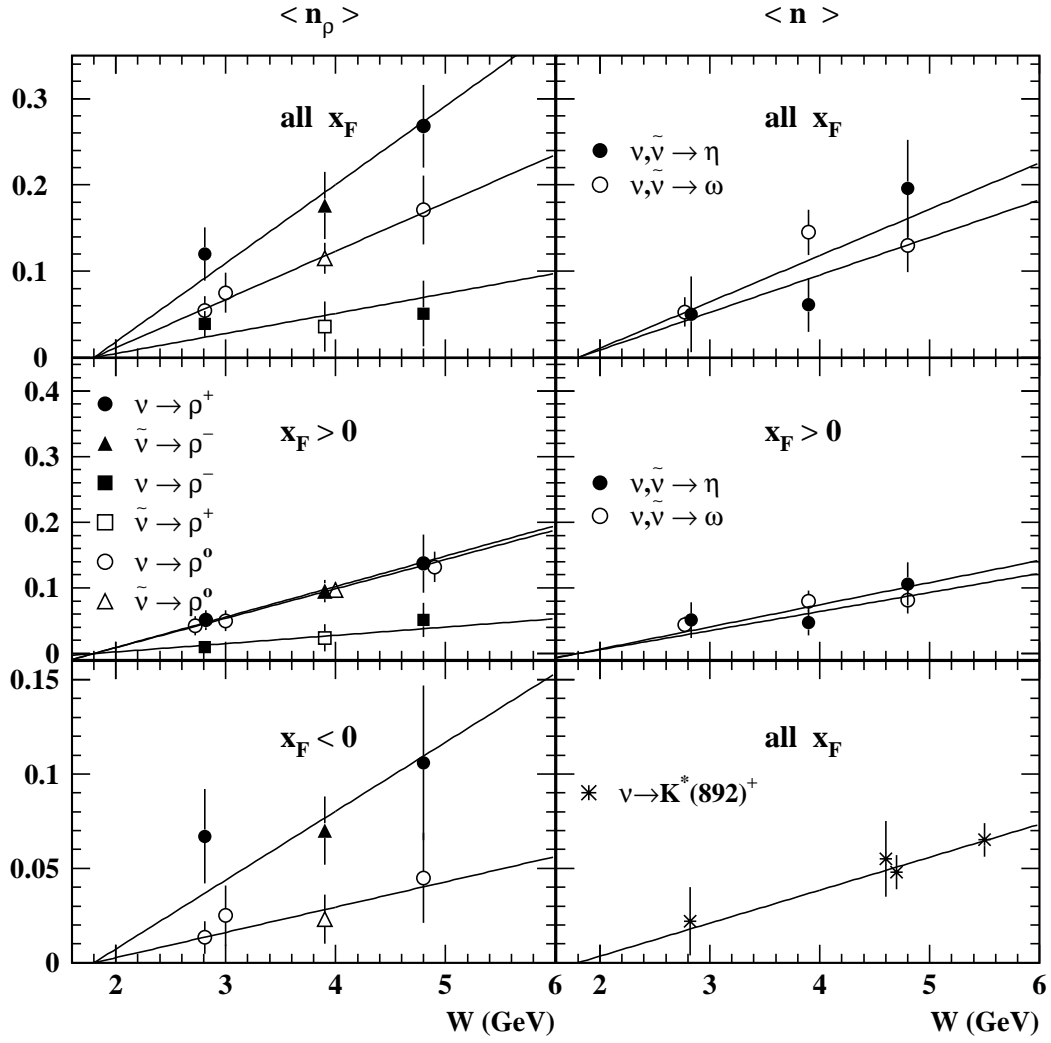


Figure 5. The  $W$ -dependence of the yields of  $\rho^0$ ,  $\rho^+$  and  $\rho^-$  (left),  $\eta$  and  $\omega$  (right: the top and middle panels) and  $K^*(892)^+$  (right: the bottom panel). The lines are the fit results (see the text).

The fitted slope parameters  $b$  are given in Table 3. It is interesting to note that the parameters  $b$  for the neutral and charged favored  $\rho$  mesons coincide at  $x_F > 0$  and significantly exceed those for  $\eta$  and  $\omega$  which, in their turn, are almost equal.

**Table 3.** The slope parameter  $b$  (in  $\text{GeV}^{-1}$ )

reaction	all $x_F$	$x_F > 0$	$x_F < 0$
$\nu(\bar{\nu}) \rightarrow \eta$	$0.044 \pm 0.011$	$0.034 \pm 0.005$	—
$\nu(\bar{\nu}) \rightarrow \rho^0$	$0.056 \pm 0.007$	$0.045 \pm 0.004$	$0.013 \pm 0.005$
$\nu \rightarrow \rho^+$ or $\bar{\nu} \rightarrow \rho^-$	$0.091 \pm 0.011$	$0.046 \pm 0.006$	$0.037 \pm 0.006$
$\nu \rightarrow \rho^-$ or $\bar{\nu} \rightarrow \rho^+$	$0.023 \pm 0.008$	—	—
$\nu(\bar{\nu}) \rightarrow \omega$	$0.054 \pm 0.007$	$0.029 \pm 0.007$	—
$\nu \rightarrow K^*(892)^+$	$0.017 \pm 0.002$	—	—

### 3.6. The Mass Dependence of the Yields of Favored Resonances at $x_F > 0$

One can expect, that the main part of the light meson resonances in the forward hemisphere is a direct product of the quark string fragmentation, with a comparatively small contribution from the decay of higher mass resonances. Furthermore, their yields in the forward hemisphere are less influenced by the intranuclear secondary interactions, in particular by interactions of pions leading to an additional production of resonances at  $x_F < 0$  (see [4] for the case of  $\rho^0$  meson). Hence the data on the mass dependence of the resonance yields at  $x_F > 0$  provide an almost non-deteriorated information on the dynamics of the quark string fragmentation. The yields of favored resonances at  $x_F > 0$ , normalized to the spin factor  $(2J + 1)$ , as a function of the resonance mass  $m_R$  are plotted in Figure 6 ( $\langle W \rangle = 2.8$  GeV, the upper panel), together with the data ( $\langle W \rangle = 3.9, 4.8$  GeV) of work [2] which include also the tensor  $f_2(1270)$  meson. Note, that the scaling to the spin factor is introduced in view of rather small spin alignment effects in the production of vector mesons ([7] and references therein). As it is seen from Figure 6, the mass dependence of the resonance yields can be approximately described by a simple exponential form  $A \exp(-\gamma m_R)$ . with the fitted values of the slope parameter  $\gamma$  (quoted in Fig. 6) not exhibiting any significant dependence on the initial internal energy of the quark string. It might be interesting to note, that a steeper mass dependence was observed [21] in higher energy  $e^+e^-$  annihilation.

## 4. THE FRACTION OF PIONS ORIGINATING FROM THE DECAY OF LIGHT RESONANCES

The presented data on resonances mean multiplicities (Table 2) allow one to estimate the fractions of  $\pi^0, \pi^-$  and  $\pi^+$  originating from the decay of light resonances. These fractions were calculated using the corresponding decay fractions [13]. To avoid double account, the contributions from the indirect  $\eta, \rho, \omega$  (from the  $\eta'$  and  $\phi$  decays) were not accounted for. The total yield of pions were taken from our work [5]. The calculated individual and summary fractions of decay pions are collected in Table 4. As it is seen,

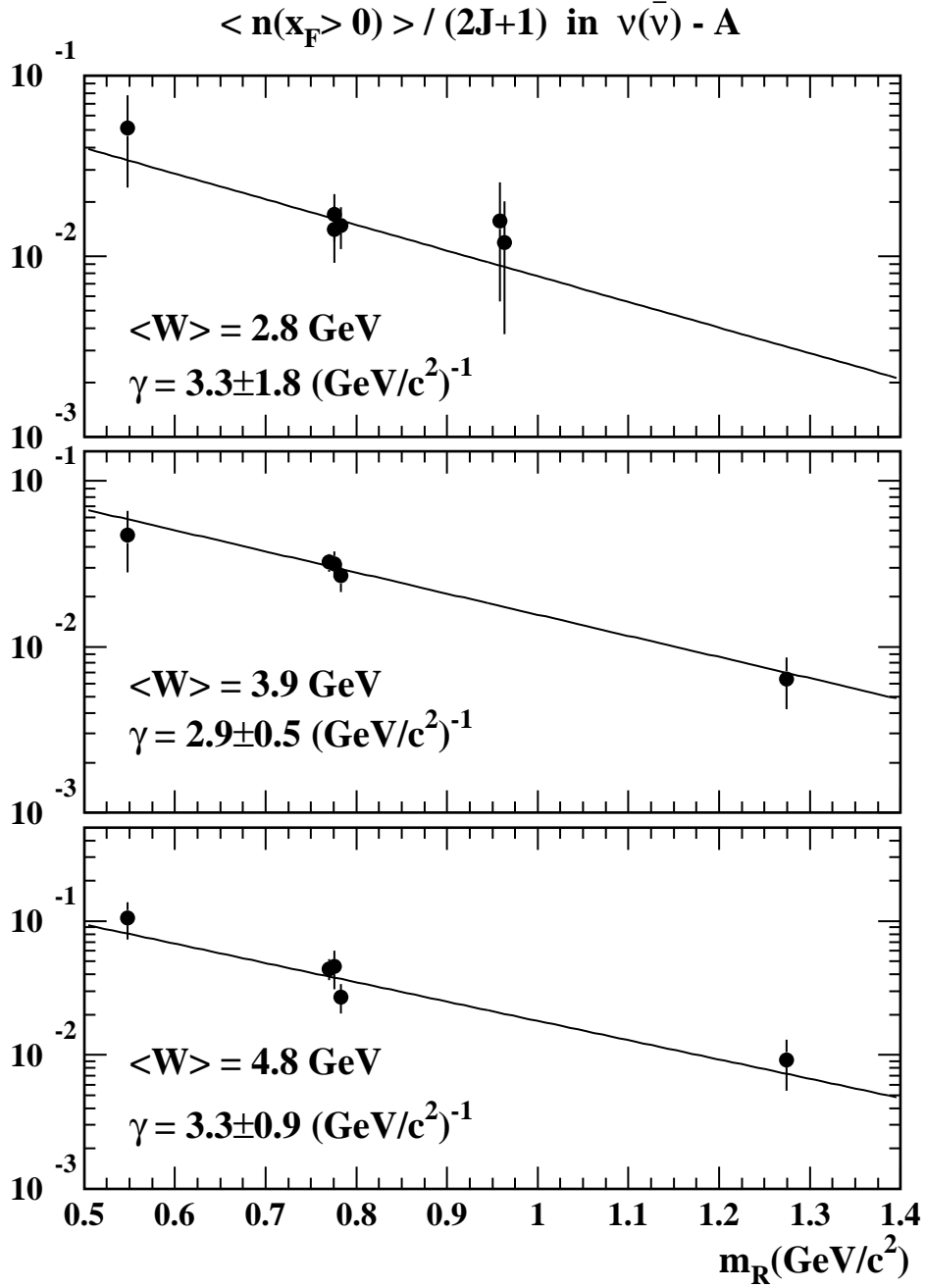


Figure 6. The mass dependence of the resonance yields, normalized to the spin factor  $(2J + 1)$ , in the forward hemisphere in  $\nu(\bar{\nu})A$  interactions. The lines are the fit results (see text).

the fractions of decay  $\pi^0$  and  $\pi^-$  are compatible, consisting about  $1/3$ , while that for  $\pi^+$  is significantly smaller, about  $1/5$ .

**Table 4.** The mean multiplicities of pions (1st row), resonances (1st column) and the fraction of pions originating from the resonance decays (in %) at  $\langle W \rangle = 2.8$  GeV. To avoid double account, the contribution of  $\eta$ ,  $\rho$ ,  $\omega$  from decays of  $\eta'$  and  $\phi$  is not included

	total	$\pi^0$ 0.904±0.066	$\pi^-$ 0.652±0.010	$\pi^+$ 1.55±0.06
$\eta$	0.050±0.044	6.65±5.85	2.10±1.85	0.88±0.78
$\rho^0$	0.054±0.017	–	8.28±2.58	3.50±1.09
$\rho^+$	0.120±0.031	13.27±3.56	–	7.74±2.02
$\rho^-$	0.039±0.015	4.41±1.73	5.98±2.30	–
$\omega$	0.053±0.017	5.75±1.84	7.38±2.37	3.10±1.00
$\eta'(958)$	0.025±0.020	1.13±0.90	2.78±2.22	1.17±0.93
$K^*(892)^0$	0.023±0.013	0.85±0.49	2.18±1.26	–
$\bar{K}^*(892)^0$	0.015±0.010	0.57±0.38	–	0.66±0.45
$K^*(892)^+$	0.022±0.012	0.81±0.47	–	0.95±0.52
$K^*(892)^-$	0.006±0.005	0.20±0.17	0.56±0.47	–
$f_0(980)$	0.014±0.010	1.03±0.73	1.42±1.00	0.60±0.42
$\phi$	0.009±0.006	0.05±0.03	0.06±0.05	0.03±0.02
	sum	34.7±7.6%	31.2±5.7%	18.4±3.0%

The  $W$ -dependence of the decay fraction can be obtained for pions from the decay of the lightest non-strange resonances ( $\eta, \rho, \omega$ ) which provide the main contribution to the decay pions (cf. Table 4) and for which the data at higher energies are available [2]. This dependence is plotted in Figure 7, where the corresponding fractions obtained in  $pp$  interactions at  $W = 27.5$  GeV [23] and in  $e^+e^-$  annihilation at 91 GeV ([13], page 330) are also shown for comparison. As it is seen, the decay fractions are continuously increased with energy.

## 5. SUMMARY

The total yields of light meson resonances (up to mass  $\sim 1$  GeV/ $c^2$ , including  $\phi$  meson) are measured in neutrino-nucleus reactions at  $\langle E_\nu \rangle \approx 10$  GeV ( $\langle W \rangle = 2.8$  GeV). For some resonances, the differential yields in the forward ( $x_F > 0$ ) and backward ( $x_F < 0$ ) hemispheres in the hadronic c.m.s. are also obtained. The data on the inclusive  $\phi$  neutrino production is obtained for the first time. It has been shown that the production of favored resonances (which can contain the current quark) occurs predominantly in the forward hemisphere, except for  $\rho^+$  meson the yield of which at  $x_F < 0$  slightly exceeds that at  $x_F > 0$ . On the contrary, the production of unfavored resonances occurs mainly at  $x_F < 0$ .

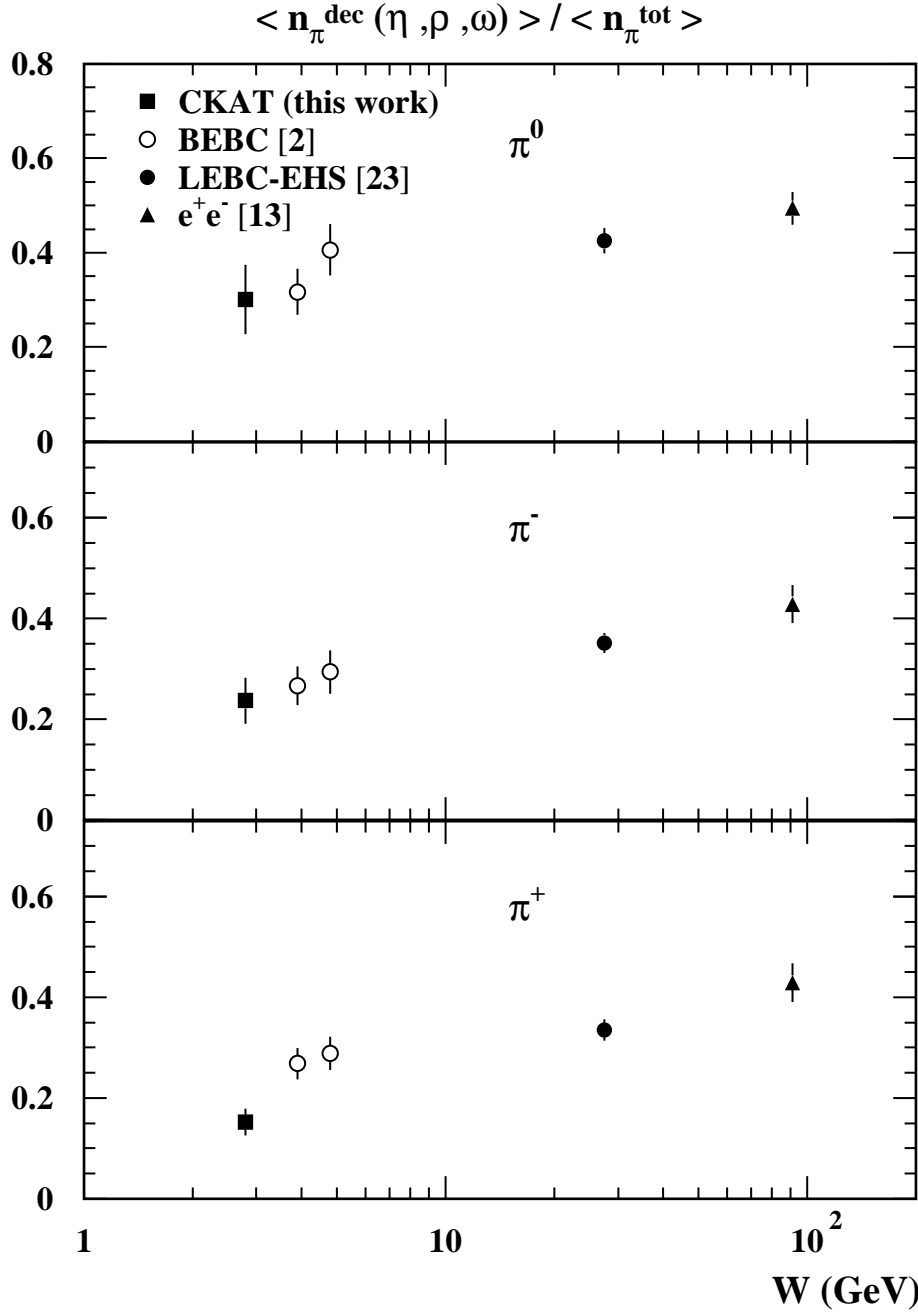


Figure 7. The fraction of pions originating from the  $\eta, \rho, \omega$  decays. The data at  $W = 3.9$  GeV for  $\pi^+(\pi^-)$  in  $\bar{\nu}Ne$  interactions [2] are replaced by those for  $\pi^-(\pi^+)$ .

An exception is  $\phi$  meson the production of which occurs practically only in the forward hemisphere.



It is shown from the combined analysis of the obtained and existing data, that the yields of resonances increase with  $W$  approximately linearly, in the range of  $W < 10$  GeV.

The yields of favored resonances at  $x_F > 0$ , normalized to the spin factor  $(2J + 1)$ , are found to be exponentially falling as a mass function.

The fractions of  $\pi^0$ ,  $\pi^-$  and  $\pi^+$  originating from the light resonance decays are estimated to be  $34.7 \pm 7.6$ ,  $31.2 \pm 5.7$  and  $18.4 \pm 3.0\%$ , respectively.

## ACKNOWLEDGMENTS

The authors from YerPhI acknowledge the supporting grants of Calouste Gulbenkian Foundation and Swiss Fonds Kidagan. The activity of one of the authors (H.G.) is supported by Cooperation Agreement between DESY and YerPhI signed on December 6, 2002.

## References

- [1] V. V. Ammosov *et al.*, *Yad. Fiz.* **46**, 131 (1987).
- [2] W. Wittek *et al.*, *Z. Phys. C* **44**, 175 (1989).
- [3] P. Astier *et al.*, *Nucl. Phys. B* **601**, 3 (2001).
- [4] N. M. Agababyan *et al.*, *Yad. Fiz.* **70**, 1948 (2007).
- [5] N. M. Agababyan *et al.*, Preprint No.1614, YerPhI (Yerevan, 2007).
- [6] N. M. Agababyan *et al.*, *Yad. Fiz.* **70**, 1786 (2007).
- [7] A. Chukanov *et al.*, *Eur. Phys. J. C* **46**, 69 (2006).
- [8] V. V. Ammosov *et al.*, *Fiz. Elem. Chastits At. Yadra* **23**, 648, 1992.
- [9] N. M. Agababyan *et al.* *Yad. Fiz.* **66**, 1350 (2003).
- [10] N. M. Agababyan *et al.*, Preprint No.1578, YerPhI (Yerevan, 2002).
- [11] N. M. Agababyan *et al.*, *Yad. Fiz.* **68**, 1209 (2005).
- [12] J. D. Jakson, *Nuovo Cim.* **34**, 1644 (1964).
- [13] Review of Particle Physics, *J. Phys. G: Nucl. Part. Phys.* **33** (2006).
- [14] R. Grässler *et al.*, *Nucl. Phys. B* **194**, 1 (1982).
- [15] V. V. Ammosov *et al.*, *Z. Phys. C* **30**, 183 (1986).
- [16] G. T. Jones *et al.*, *Z. Phys. C* **57**, 197 (1993).
- [17] G. T. Jones *et al.*, *Z. Phys. C* **27**, 43 (1985).
- [18] A. Wroblewski, *Acta Phys. Pol.* **16**, 379 (1985).
- [19] W. Hofmann, *Nucl. Phys. A* **479**, 337 c (1988).
- [20] A. Wroblewski, IFD-10-1990; Plenary talk given at 25 th Int. Conf. on High Energy Physics, Singapore, Aug 2-8, 1990.
- [21] P. V. Chliapnikov, *Phys. Lett. B* **462**, 341 (1999).
- [22] A. E. Asratyan *et al.*, *Phys. Lett. B* **257**, 525 (1991).
- [23] M. Aguilar-Benitez *et al.*, *Z.Phys. C* **50**, 405 (1991).

*Received April 6, 2010.*

Препринт отпечатан с оригинала-макета, подготовленного авторами.

Н.М. Агабабян, Н. Григорян, А.А. Иванилов и др.

Выходы легких мезонных резонансов в нейтрино-ядерных взаимодействиях при  $\langle E_\nu \rangle \approx 10$  ГэВ.

Оригинал-макет подготовлен с помощью системы **Л<sup>A</sup>T<sub>E</sub>X**.

---

Подписано к печати 15.04.2010. Формат  $60 \times 84/16$ . Офсетная печать.  
Печ.л. 1,062. Уч.-изд.л. 1,632. Тираж 80. Заказ 33. Индекс 3649.

---

ГНЦ РФ Институт физики высоких энергий  
142281, Протвино Московской обл.

Индекс 3649

---

П Р Е П Р И Н Т 2010–4,            И Ф В Э,            2010

---